

Synthesis, Spectroscopy, and Structure of a Family of Iridabenzenes Generated by the Reaction of Vaska-Type Complexes with a Nucleophilic 3-Vinyl-1-cyclopropene[†]

Robert D. Gilbertson, Thomas L. S. Lau, Seren Lanza, He-Ping Wu, Timothy J. R. Weakley,[‡] and Michael M. Haley*

Department of Chemistry, University of Oregon, Eugene, Oregon 97403-1253

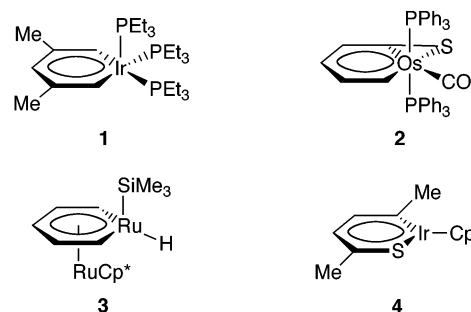
Received May 27, 2003

Seven new iridabenzenes were prepared by the addition of (*Z*)-1,2-diphenyl-3-(2-lithioethenyl)-1-cyclopropene to the Vaska-type complexes [IrCl(CO)(PR₃)₂], containing differing phosphine ligands. The iridabenzenes could be isolated from the reaction mixture either by direct means or after heating of the crude solution. In the case of the reactions using PMe₃ and PEt₃, a σ -vinyl/ η^2 -cyclopropene Ir(I) complex, best described as an iridabenzvalene, could be isolated and fully characterized. The metallabenzvalene intermediate could be cleanly converted to the corresponding iridabenzene by heating in solution. The PEt₃-substituted iridabenzene and iridabenzvalene were characterized by X-ray crystallography. Plausible mechanisms for the formation of both iridacycles from the lithiated vinylcyclopropene as well as the isomerization of the benzvalene into the benzene are postulated.

Introduction

As a conceptual cornerstone in modern chemistry, aromaticity has been extensively studied since the discovery of benzene nearly 175 years ago.¹ Aromaticity, however, is not limited solely to hydrocarbon structures. A variety of molecules that incorporate other atoms as part of the six-membered ring have been shown to exhibit stabilization due to aromatic ring currents. Among these are neutral systems such as pyridine and phosphabenzene, as well as charged species such as boratabenzene and the pyrylium ion.¹ In each of the aforementioned examples, one of the methine (CH) units in benzene was replaced with an isolobal heteroatomic fragment; nevertheless, the molecules retained aromatic chemical and physical properties.

In their seminal paper from 1979, Thorn and Hoffmann² predicted that analogous replacement of a benzene CH moiety with an isolobal transition-metal fragment (ML_n) would result in the formation of a new class of aromatics: *metallabenzenes*.³ Metallabenzenes differ from regular aromatics in that π bonding requires involvement of the metal d orbitals, as the metal p orbitals participate in σ -bonding to the ligands.^{2,3} Thus, as organic/transition-metal “hybrids”, one would expect metallabenzenes to exhibit physical and chemical prop-



erties from both areas. Indeed, iridabenzene **1**, the best studied metallaaromatic, shows many similarities to heterobenzenes—downfield chemical shifts for ring protons, ring planarity, delocalized bonding, arene displacement from (arene)Mo complexes, etc.⁴ The transition-metal center, however, exerts significant influence on the chemistry of the system by undergoing oxidative addition, ligand dissociation, and electron-transfer processes.⁴ Only recently was it shown that the metallabenzene skeleton can undergo electrophilic aromatic substitution.⁵

Over the subsequent 24 years since the initial proposal, approximately 25 varieties of metallaaromatic species have been isolated and/or characterized (e.g., **1–4**).^{3–8} Of this number though, only two families, namely **1**⁴ and **2**,⁵ can be considered ideally as discrete metallabenzenes. The remaining examples either have been stabilized by η^6 coordination of the metallacyclic ring to a second transition-metal complex (e.g., **3**)⁶ or have incorporated a heteroatom (S, N, O) in the metallacyclic backbone (e.g., **4**).⁷ While the preparation of

* To whom correspondence should be addressed. E-mail: haley@oregon.uoregon.edu.

[†] Metallabenzenes and Valence Isomers. 6. Part 5: Reference 12c.

[‡] To whom inquiries about the X-ray crystal structures should be addressed.

(1) (a) Garratt, P. J. *Aromaticity*; Wiley: New York, 1986. (b) Minkin, V. I.; Glukhovtsev, M. N.; Simkin, B. Ya. *Aromaticity and Antiaromaticity*; Wiley: New York, 1994. (c) *Aromaticity*. *Chem. Rev.* **2001**, *101*(5).

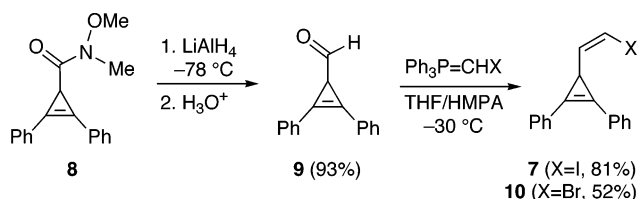
(2) (a) Thorn, D. L.; Hoffmann, R. *Nouv. J. Chim.* **1979**, *3*, 39–45. See also: (b) Iron, M. A.; Martin, J. M. L.; van der Boom, M. E. *Chem. Commun.* **2003**, 132–133. (c) Effertz, U.; Englert, U.; Podewils, F.; Salzer, A.; Wagner, T.; Kaupp, M. *Organometallics* **2003**, *22*, 264–274.

(3) Bleeke, J. R. *Chem. Rev.* **2001**, *101*, 1205–1227.

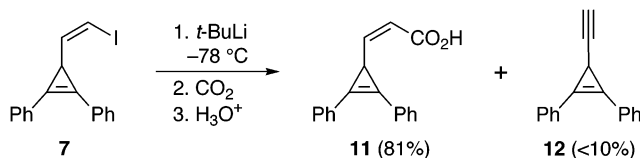
(4) Bleeke, J. R.; Behm, R.; Xie, Y.-F.; Chiang, M. Y.; Robinson, K. D.; Beatty, A. M. *Organometallics* **1997**, *16*, 606–623.

(5) (a) Elliot, G. P.; Roper, W. R.; Waters, J. M. *J. Chem. Soc., Chem. Commun.* **1982**, 811–813. (b) Elliot, G. P.; Mcauley, N. M.; Roper, W. R. *Inorg. Synth.* **1989**, *26*, 184–189. (c) Rickard, C. E. F.; Roper, W. R.; Woodgate, S. D.; Wright, L. J. *Angew. Chem., Int. Ed.* **2000**, *39*, 750–752.

Scheme 2



Scheme 3

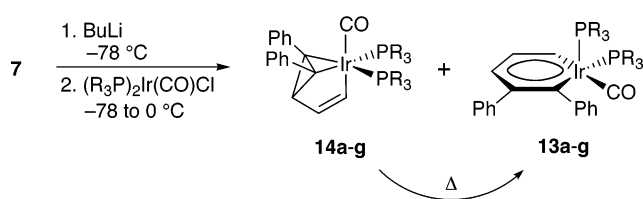


ture with LiAlH_4 gave aldehyde **9** in 93% yield. The Wittig reaction of **9** with bromomethyltriphenylphosphorane²⁰ furnished cyclopropene **10** in 52% yield; however, the poor 5:4 *Z:E* stereoselectivity of the reaction (as determined by ^1H NMR integration) precluded utilization of this molecule. Gratifyingly, use instead of iodomethyltriphenylphosphorane²¹ provided cyclopropene **7** in 81% yield with high stereoselectivity (>20:1 *Z:E*). Ligand **7** can be prepared in gram quantities; however, the molecule is somewhat unstable and should be stored in the dark at $-20\text{ }^\circ\text{C}$ with a small amount of hydroquinone to inhibit decomposition.

Before committing to metallacycle synthesis, we needed to address lingering concerns that the (β -halovinyl)cyclopropene might undergo a competitive elimination reaction in addition to lithium/halogen exchange, as well as potentially isomerize from *Z* to *E* under the reaction conditions. Treatment of **7** with *t*-BuLi at $-78\text{ }^\circ\text{C}$ followed by bubbling dry CO_2 through the solution gave, after workup and recrystallization, carboxylic acid **11** in 81% yield along with a small amount (<10%) of alkyne **12**,^{18c} the product of HI elimination (Scheme 3). This latter material could be suppressed by switching to BuLi without decreasing the yield of **11**. Importantly, the *Z* geometry of the double bond was retained using either base, as indicated by the coupling constant of the alkene hydrogens ($J = 11.4\text{ Hz}$).

Metallacycle Formation. Although other transition metals were considered, Ir(I) was chosen as the focus of our initial investigations, given the extensive success the Bleeke group has enjoyed in their iridaaromatic studies.^{3,4} We decided upon Vaska-type complexes as the source of Ir(I) because (1) such starting organometallic complexes either are commercially available or are easily prepared,²² (2) the reaction of vinyl lithiates with

Scheme 4



Vaska's complex is known to produce stable σ -vinyl species that do not undergo β -hydride elimination or migratory insertion of CO at room or slightly higher temperature,²³ and (3) both the starting Vaska and intermediate σ -vinyl complexes are coordinatively unsaturated and should react readily with the strained cyclopropene to form $18e^-$ species.

Lithium-iodine exchange of **7** with 1 equiv of BuLi at $-78\text{ }^\circ\text{C}$, followed by trapping of the intermediate vinyl lithiate with $\text{IrCl}(\text{CO})(\text{PPh}_3)_2$, directly resulted in formation of iridabenzene **13a** (Scheme 4). When the initial suspension was slowly warmed to $0\text{ }^\circ\text{C}$, a color change from yellow to red-orange was observed. Excess lithiate was quenched with CHCl_3 ,²⁴ and the insoluble salts were removed by filtration through a glass frit. After removal of solvent, the crude reaction mixture was dissolved in a mixture of toluene and hexanes (1:1) at room temperature. Upon cooling to $-35\text{ }^\circ\text{C}$, **13a** crystallized as X-ray-quality red prisms in 66% yield.

Repetition of the above reaction sequence with Vaska-type complexes possessing alkyl-containing phosphines produced a surprising second product. In contrast to the preparation of **13a**, the crude mixture from the reaction of lithiated **7** with $\text{IrCl}(\text{CO})(\text{PEt}_3)_2$ showed no evidence of a metallabenzene product in the ^1H NMR spectrum. The crude orange oil was taken up in ether, filtered, and cooled to $-35\text{ }^\circ\text{C}$, whereupon light yellow crystals formed in 51% yield. The NMR spectral data obtained from the recrystallized product suggested formation of the σ -vinyl/ η^2 -cyclopropene complex "iridabenzvalene"²⁵ **14d** (Scheme 4). Other phosphines provided mixtures of **13** and **14**, which were then converted to exclusively **13** simply by heating. Similarly, heated solutions of pure **14** cleanly and quantitatively isomerized to **13**. The results utilizing the various phosphines are summarized in Table 1. Whereas **14b** and **14d** could be isolated in pure form, the remaining η^2 complexes either isomerized on attempted separation/purification (**14c** and **14e**) or were thermally labile at room temperature and thus rearranged rapidly (**14f**). It is interesting to note that η^2 complexes **14a** and **14g** were never observed in the crude reaction mixtures. PPh_3 and $\text{P}(p\text{-MeOPh})_3$, both of which possess a cone angle of 145° ,²⁶ appear to be the upper limit of usable phosphine ligands in the Ir(I) species, as utilization of Vaska-type complexes with bulkier phosphines such as $\text{P}(i\text{-Pr})_3$ (cone angle 160°) and PCy_3 (cone angle 170°) failed to give metallacyclic

(18) (a) Haley, M. M.; Biggs, B.; Looney, W. A.; Gilbertson, R. D. *Tetrahedron Lett.* **1995**, *36*, 3457–3460. (b) Gilbertson, R. D.; Haley, M. M.; Weakley, T. J. R.; Weiss, H.-C.; Boese, R. *Organometallics* **1998**, *17*, 3105–3107. (c) Gilbertson, R. D.; Weakley, T. J. R.; Haley, M. M. *J. Org. Chem.* **2000**, *65*, 1422–1430. (d) Gilbertson, R. D.; Wu, H.-P.; Gorman-Lewis, D.; Weakley, T. J. R.; Weiss, H.-C.; Boese, R.; Haley, M. M. Submitted for publication. (e) Gilbertson, R. D.; Bercot, E. A.; Schill, B.; Haley, M. M. Unpublished results.

(19) Hughes, R. P.; Robinson, D. J. *Organometallics* **1989**, *8*, 1015–1019.

(20) (a) Smithers, R. H. *J. Org. Chem.* **1978**, *43*, 2833–2838. (b) Matsumoto, M.; Kuroda, K. *Tetrahedron Lett.* **1980**, *21*, 4021–4024.

(21) (a) Stork, G.; Zhao, K. *Tetrahedron Lett.* **1989**, *30*, 2173–2174. (b) Bestmann, H. J.; Rippel, H. C.; Dostalek, R. *Tetrahedron Lett.* **1989**, *30*, 5261–5262.

(22) Burk, M. J.; Crabtree, R. H. *Inorg. Chem.* **1986**, *25*, 931–932.

(23) Schwartz, J.; Hart, D. W.; McGiffert, B. *J. Am. Chem. Soc.* **1974**, *96*, 5613–5614.

(24) In our earlier reports we used EtOH to quench the reaction. This was subsequently shown to affect the ratio of **13** to **14** initially produced.

(25) For a discussion concerning the differences between the two limiting resonance forms of **14** (η^2 - π complex versus metallacyclopropene), see ref 11.

(26) Tolman, C. A. *Chem. Rev.* **1977**, *77*, 313–348.

Table 1. Phosphine Data and Yields for Iridabenzenes **13 and Iridabenzvalenes **14****

compd	phosphine	cone angle ^a	initial pdt ratio ^b	isolated yield (%)		yield (%) 14 → 13
				13	14	
13a/14a	PPh ₃	145	100:0	66		
13b/14b ^c	PMe ₃	118	0:100		54	97
13c/14c	PMe ₂ Ph	122	2:98	58		
13d/14d	PEt ₃	132	0:100		51	95
13e/14e	PMePh ₂	136	30:70	56		
13f/14f	P(<i>i</i> -Bu) ₃	143	35:65	49		
13g/14g	P(<i>p</i> -MeOPh) ₃	145	100:0	61		

^a Reference 26. ^b Ratio of **13** to **14** in the crude reaction mixture immediately after workup, as determined by ¹H NMR spectroscopy. ^c Reference 11.

products. Although iridabenzene **13a** is air stable both in the solid state and in solution, the remaining iridabenzenes, especially the trialkylphosphine-substituted systems, decompose readily upon exposure to oxygen. In contrast, samples of pure iridabenzvalenes are air-stable and can be kept for months either in solution (nondonating solvent) or in the solid state when stored at 0 °C; however, in donating solvents such as acetone, **14** readily rearranges to **13**.

Spectroscopy and Structure

Iridabenzenes. The key resonance in the ¹H NMR spectra of the iridabenzenes (Table 2) is the signal for H5, which denotes whether metallabenzene formation has indeed occurred. In CD₂Cl₂ solution this multiplet appears between 10.41 ppm (**14a**) and 11.30 ppm (**14d**). The large downfield shift, typical of all metallabenzenes,³ can be attributed primarily to the anisotropy of the large metal atom on H5. The two remaining hydrogens on the metallocyclic ring (H3 and H4) are sufficiently removed from the anisotropic influences of the iridium center and thus appear as distinct multiplets in the "normal" region for aromatic protons (7.99–7.69 ppm for H3 and 7.69–7.38 ppm for H4). Although it is difficult to discern any trends for the alkylphosphine-containing cycles, successive replacement of –Me with –Ph on the phosphine results in deshielding of H3 and H4 and shielding of H5, which for the latter case is likely attributable to the close proximity of the phosphine phenyl rings.

In the ¹³C NMR spectra of the metallacycles, the signals for C1 and C5 appear rather far downfield in the range of 176–190 ppm, whereas C2, C3, and C4 show up in the "normal" region for aromatic carbons. Like most carbons meta to a substituent that is varied, C2 and C4 are relatively insensitive ($\Delta\delta < 1.4$ ppm) when the metal's ligand sphere is altered; however, the

C5 ortho and C3 para carbons vary considerably. As before, there is little change in the ¹³C resonances of the alkylphosphine-containing cycles, yet successive replacement of –Me with –Ph on the phosphine results in deshielding of C3 ($\Delta\delta = 4.5$ ppm) and C5 ($\Delta\delta = 11$ ppm), as well as of the carbonyl carbon (C6, $\Delta\delta = 11.5$ ppm). Interestingly, C1 is rather insensitive to these changes ($\Delta\delta = -1.4$ ppm) and shows a very slight shielding. The differences in C3, C5, and C6 can be rationalized in terms of electronic influences. As the donating ability of the phosphine decreases (increasing number of –Ph substituents), the increasingly electron-deficient metal center pulls electron density out of these carbons, thus resulting in the shift to lower field. Nonetheless, this does not explain the puzzling behavior of C1. Although one would like to invoke trans influences of the phosphines, the insensitivity of the chemical shift suggests otherwise. It is possible that the phenyl substituent on C1, even though not conjugated because of its orthogonality (due to sterics), does contribute some electron density through induction and thus mitigates the influence of the phosphines.

The ³¹P NMR spectra of the iridabenzenes exhibit sharp singlets, even upon cooling to ca. –80 °C, which suggests that the cycles are stereochemically nonrigid. The axial and basal phosphines are exchanging rapidly in solution via the well-known Berry pseudorotation process;²⁷ nonetheless, the considerably smaller CO ligand is most likely spending a disproportionate amount of time in the basal site near C1, due to the much larger steric bulk of the phosphines. Such ligand site preference has been beautifully demonstrated by Bleeke et al. through careful analysis of P–H coupling constants in a similar system.⁴ This preference is also supported by the fact that ¹³C resonance for C5 is a singlet, whereas C1 couples to the phosphines and appears as a triplet.

Unambiguous confirmation of the structures of metallabenzenes **13a**¹⁰ and **13d** (Figure 1) was provided by single-crystal X-ray diffraction. These structures are similar in many respects to that reported for iridabenzene **1**, a close analogue to our metallacycles. Selected bond lengths and bond angles for all three compounds are given in Table 3. Both **13a** and **13d** possess a slightly distorted square pyramidal coordination geometry, with P1 occupying the axial site and C1, C5, C6, and P2 filling the basal sites. The metallabenzene ring is essentially planar (mean deviation 0.024 Å for **13a** and 0.041 Å for **13d**), with the iridium center tilted out of the plane of the C₅ backbone by 3.7 and 6.4° for **13a** and **13d**, respectively. Delocalization of the π system is evident in the bond lengths throughout the six-mem-

Table 2. Selected NMR and IR Spectral Data for Iridabenzenes **13^a**

compd	phosphine	¹ H NMR (δ)			¹³ C NMR (δ)						³¹ P NMR (δ)	IR ν_{CO} (cm ⁻¹)
		H3	H4	H5	C1	C2	C3	C4	C5	C6		
13a	PPh ₃	7.99	7.69	10.41	187.60	141.93	139.99	127.76	187.43	201.09	16.44	1990
13b	PMe ₃	7.75	7.49	11.10	189.25	140.49	135.53	128.65	176.58	189.44	–40.54	1962
13c	PMe ₂ Ph	7.82	7.53	11.05	188.56	140.53	136.49	128.85	179.68	190.77	–26.90	1970
13d	PEt ₃	7.69	7.40	11.30	189.87	140.53	135.67	128.07	176.45	192.36	–2.08	1967
13e	PMePh ₂	7.98	7.66	10.93	187.36	141.47	137.61	128.37	181.93	197.14	–5.20	1979
13f	P(<i>i</i> -Bu) ₃	7.71	7.51	10.89	190.54	141.45	136.14	128.01	177.28	194.09	–0.29	1958
13g	P(<i>p</i> -MeOPh) ₃	7.96	7.38	10.43	188.51	141.70	138.92	128.50	187.11	198.18	13.01	1973

^a All NMR data were acquired in CD₂Cl₂. ¹H and ¹³C assignments were confirmed by HMBC and HMQC experiments. Atom labeling is as shown in Figure 1.

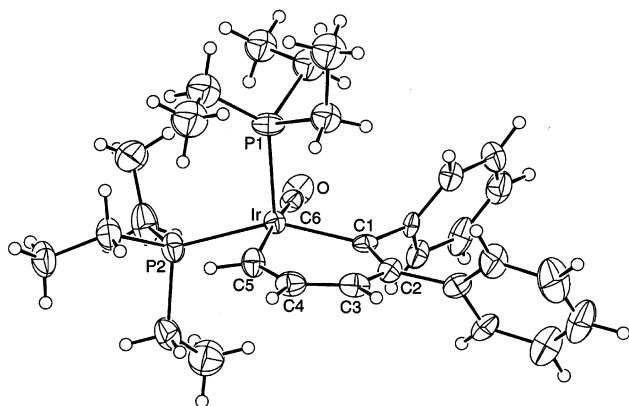


Figure 1. Molecular structure of iridabenzene **13d**. Ellipsoids are drawn at the 30% probability level.

Table 3. Selected Bond Lengths (Å) and Angles (deg) for Iridabenzenes 1, 13a, and 13d

	1 ^a	13a ^b	13d
Ir–P1	2.268(2)	2.317(2)	2.285(3)
Ir–P2	2.374(2) ^c	2.373(2)	2.366(3)
Ir–C1	2.024(8)	2.021(8)	2.048(9)
Ir–C5	1.985(8)	2.025(8)	2.004(10)
Ir–C6	<i>d</i>	1.925(9)	1.887(11)
C1–C2	1.369(10)	1.409(11)	1.427(12)
C2–C3	1.402(11)	1.410(12)	1.372(14)
C3–C4	1.370(11)	1.377(13)	1.386(15)
C4–C5	1.392(10)	1.334(12)	1.381(13)
C6–O	<i>d</i>	1.140(10)	1.154(11)
P1–Ir–P2	104.0(1) ^c	99.2(1)	104.8(1)
P1–Ir–C1	103.7(2)	112.6(2)	101.9(2)
P1–Ir–C5	90.6(2)	95.4(3)	94.9(3)
P1–Ir–C6	<i>d</i>	99.3(3)	96.9(3)
P2–Ir–C1	163.8(2)	148.2(2)	153.0(2)
P2–Ir–C5	87.5(2) ^c	90.6(3)	85.6(3)
C5–Ir–C6	<i>d</i>	165.0(4)	167.8(4)
C1–Ir–C5	84.7(3)	86.9(3)	88.1(4)
Ir–C1–C2	131.2(6)	128.8(6)	127.1(7)
Ir–C1–C7	<i>d</i>	118.5(5)	117.2(6)
C1–C2–C3	122.6(7)	123.6(8)	123.1(10)
C2–C3–C4	125.3(7)	124.2(8)	127.9(10)
C3–C4–C5	121.8(7)	125.5(8)	122.5(10)
C4–C5–Ir	132.9(6)	130.7(7)	130.4(8)
tilt angle ^e	9.2	3.7	6.4

^a Reference 4. ^b Reference 10. ^c Average value. ^d No comparable value. ^e The angle between plane 1 (C1, Ir, C5) and plane 2 (C1, C2, C3, C4, C5).

bered ring. The Ir–C1 (2.048(9) Å) and Ir–C5 (2.004(10) Å) bonds in **13d**, which are intermediate between typical Ir–C single and double bonds, are similar in length. The carbon–carbon bonds of the metallacycles are typical of benzene derivatives (average 1.383 and 1.392 Å for **13a** and **13d**, respectively). To accommodate the long Ir–C bonds in the six-membered ring, the C1–Ir–C5 angle is constrained to 88.1° in **13d** and the remaining bond angles in the metallacycle are expanded by 3.1–10.4° over the typical sp² carbon angle of 120° (Table 3).

Iridabenzvalenes. Due to the instability of **14c**, **14e**, and **14f**, only partial NMR data could be obtained; however, complete NMR data for **14b** and **14d** were secured. The diagnostic peak in the proton spectra of the iridabenzvalenes is a broad singlet (multiplet) centered around 3.8 ppm, corresponding to the bridgehead cyclopropyl proton (H3). Alkene H4 appears as a multiplet near 6.8 ppm, with H5 typically obscured underneath phenyl resonances around 7.1 ppm. The C_{2v} symmetry of the molecules is reflected in the equiva-

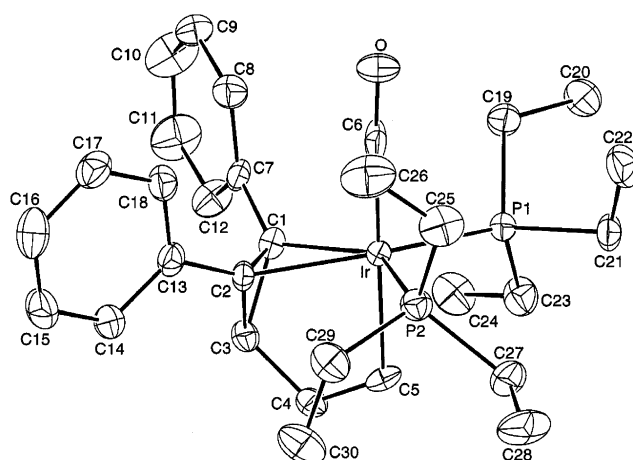


Figure 2. Molecular structure of iridabenzvalene **14d**. Ellipsoids are drawn at the 30% probability level.

lence of the two phenyl rings on the η²-coordinated cyclopropene in both the ¹H and ¹³C NMR spectra. One of the most noticeable changes from **7** is the marked upfield shift (Δδ > 45 ppm) of the cyclopropenyl carbons, which typically appear around 110 ppm. This two-carbon resonance now occurs at ca. 60 ppm, indicating strongly the increased p character of the carbon and thus significant relief of ring strain. All of the spectroscopic data support a trigonal-bipyramidal arrangement of the ligands around the Ir center.

The structures of **14b**¹¹ and **14d** (Figure 2) were also confirmed by single-crystal X-ray diffraction. Selected bond lengths and bond angles for both compounds are given in Table 4. The axis of the olefinic cyclopropene bonds in **14b/14d** is oriented in the equatorial plane of the complex, which is typical of trigonal-bipyramidal d⁸ complexes.²⁷ The Ir–C(1) (2.172(11) Å) and Ir–C(2) (2.159(9) Å) bond lengths of **14d** are slightly longer than the corresponding bond lengths in a closely related “iridabicyclo[1.1.0]butane” (2.116/2.118 Å).^{15f} The length of the C(1)–C(2) bond (1.440(16) Å) in **14d** is increased relative to a typical cyclopropene (~1.29 Å)²⁸ and is characteristic of transition-metal olefin complexes that have a significant back-bonding contribution from the metal center.²⁷ Most other aspects of the structure of **14d** are strictly analogous to those of **14b**, which have been described in detail.¹¹

Reactivity

Given the similarities between **1** and **13**, the reaction chemistry of our iridabenzenes has received only cursory examination. In addition to undergoing [4 + 2] cycloadditions with maleic anhydride and dimethyl maleate, the iridabenzenes react with atmospheric oxygen to produce dioxygen-bridged complexes. The exception to this reactivity was **13a**, which required elevated temperatures before the onset of cycloaddition. In the case of **13b**, exposure of the deep red solution to air resulted

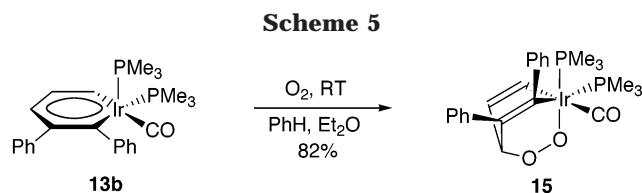
(27) (a) Housecroft, C. E.; Sharpe, A. G. *Inorganic Chemistry*, Prentice Hall: London, 2001. (b) Spessard, G. O.; Miessler, G. L. *Organometallic Chemistry*, Prentice Hall: London, 1997. (c) Collman, J. P.; Hegedus, L. S.; Norton, J. R.; Finke, R. G. *Principles and Applications of Organotransition Metal Chemistry*, University Science Books: Mill Valley, CA, 1987.

(28) Boese, R. In *Advances in Strain in Organic Chemistry*; Halton, B., Ed.; JAI Press: London, 1992; Vol. 2, pp 191–254.

Table 4. Selected Bond Lengths (Å) and Angles (deg) for Iridabenzvalenes 14b and 14d

	14b ^a	14d
Ir–P1	2.306(3)	2.330(3)
Ir–P2	2.318(3)	2.326(3)
Ir–C1	2.146(10)	2.172(11)
Ir–C2	2.143(8)	2.159(9)
Ir–C5	2.095(11)	2.092(11)
Ir–C6	1.870(10)	1.865(11)
C1–C2	1.447(12)	1.440(16)
C1–C3	1.529(12)	1.519(15)
C2–C3	1.526(12)	1.533(15)
C3–C4	1.466(13)	1.481(16)
C4–C5	1.322(13)	1.328(15)
C6–O	1.147(10)	1.155(13)
P1–Ir–P2	104.1(1)	109.4(1)
P1–Ir–C1	109.4(2)	106.5(3)
P1–Ir–C5	86.4(3)	86.8(3)
P1–Ir–C6	92.6(3)	90.8(4)
P2–Ir–C2	105.9(3)	104.0(3)
C1–Ir–C2	39.4(3)	38.8(4)
C5–Ir–C6	178.9(4)	176.5(5)
C1–Ir–C5	83.1(4)	82.8(5)
Ir–C1–C2	70.2(5)	70.1(6)
Ir–C2–C1	70.4(5)	71.0(6)
C1–C3–C2	56.5(5)	56.3(7)
C1–C3–C4	116.4(8)	118.0(9)
C2–C3–C4	116.4(8)	116.5(9)
C3–C4–C5	115.5(9)	113.7(10)
C4–C5–Ir	111.4(7)	113.1(8)
dihedral angle ^b	116.3(2)	116.2(2)

^a Reference 11. ^b The angle between plane 1 (C1, C2, C3) and plane 2 (C7, C1, C2, C13).



in rapid discoloration to pale yellow, and compound **15** could be isolated in 82% yield (Scheme 5) as yellow crystals.

The X-ray structure of **15** is shown in Figure 3; selected bond lengths and bond angles as well as comparison with the dioxygen adduct of **1**²⁹ are given in Table 5. As depicted in Figure 3, the oxygen has added across the bottom face of the square-pyramidal geometry of **13b**, leading to an octahedral adduct that is reminiscent of the bicyclo[2.2.0]octadiene skeleton. Unlike the all-carbon analogue, the considerably longer Ir–C and Ir–O bonds help alleviate much of the strain in the bicyclic system. As before, the small CO ligand is in a cis relationship with C1. The stereochemical rigidity of the skeleton is reflected in the ³¹P NMR data, where the nonequivalent phosphines appears as two doublets.

Mechanisms for Metallacycle Formation and Iridabenzvalene Isomerization

A likely reaction pathway for metallacycle formation is shown in Scheme 6. Initial substitution of the chloride ligand by lithiate **16** should give the σ -vinyl complex **17**. Although we have never observed **17** (despite efforts

(29) Blecke, J. R.; Xie, Y.-F.; Bass, L.; Chiang, M. Y. *J. Am. Chem. Soc.* **1991**, *113*, 4703–4704.

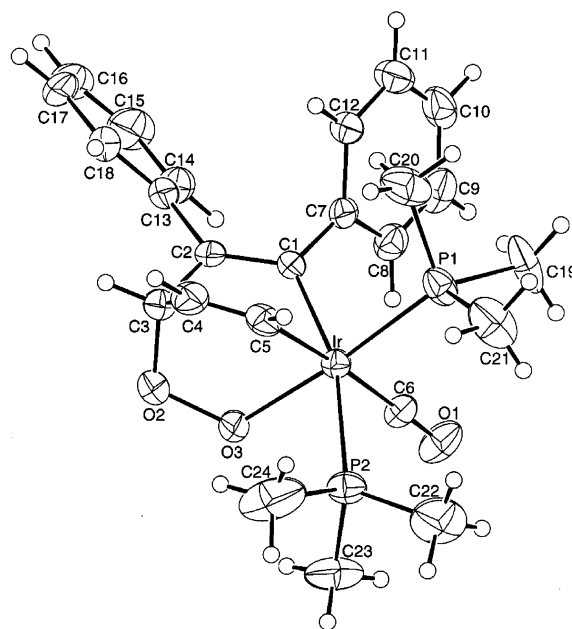


Figure 3. Molecular structure of cycloadduct **15**. Ellipsoids are drawn at the 30% probability level.

Table 5. Selected Bond Lengths (Å) and Angles (deg) for Dioxygen Cycloadducts 1·O₂ and 15

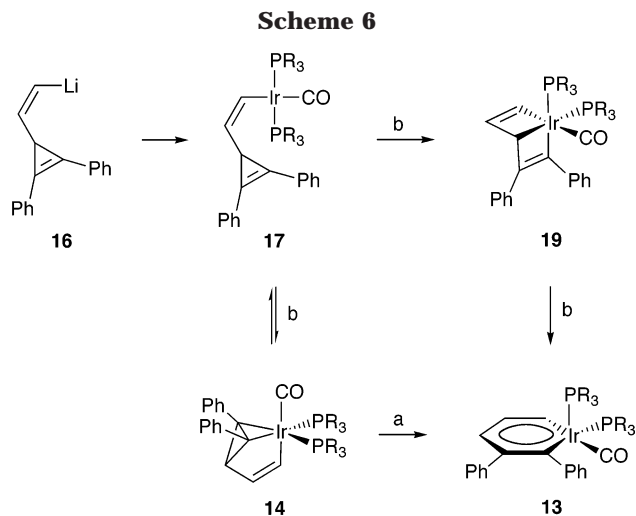
	1·O ₂ ^a	15
Ir–P1	2.279(3)	2.283(2)
Ir–P2	2.387(2)	2.395(2)
Ir–O3	2.111(6)	2.089(4)
Ir–C1	2.075(8)	2.118(6)
Ir–C5	2.062(8)	2.068(7)
Ir–P3(C6) ^b	2.395(2)	1.908(7)
C1–C2	1.315(11)	1.342(8)
C2–C3	1.512(11)	1.512(9)
C3–C4	1.521(13)	1.504(11)
C4–C5	1.339(12)	1.292(9)
C6–O1	^c	1.122(7)
O2–O3	1.466(7)	1.464(6)
O2–C3	1.435(10)	1.427(7)
P1–Ir–P2	97.5(1)	102.7(1)
P1–Ir–O3	171.8(1)	174.7(1)
P1–Ir–C1	92.5(2)	92.2(2)
P1–Ir–C5	87.7(3)	87.5(2)
P1–Ir–P3(C6) ^b	102.9(1)	95.0(2)
P2–Ir–C1	169.2(2)	163.5(2)
P2–Ir–C5	90.2(2)	86.8(2)
C5–Ir–P3(C6) ^b	166.9(3)	176.2(3)
C1–Ir–C5	86.2(3)	86.7(3)
Ir–C1–C2	119.9(6)	115.3(5)
Ir–C1–C7	^c	123.8(4)
C1–C2–C3	118.0(7)	119.5(6)
C2–C3–C4	110.2(7)	111.7(6)
C3–C4–C5	119.0(7)	119.3(7)
C4–C5–Ir	118.4(7)	118.4(6)

^a Reference 29. ^b P3 in **1**·O₂, C6 in **15**. ^c No comparable value.

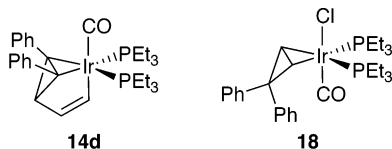
to do so),³⁰ such σ -bound species are known^{23,31} and in the case of Pt(II) two have been characterized crystallographically with this exact vinylcyclopropene ligand.^{12d} η^2 coordination of the π bond of the tethered cyclopropene unit to the metal center furnishes benzvalene **14**.

(30) Gilbertson, R. D. Ph.D. Thesis, University of Oregon, 1999.

(31) (a) Wiedemann, R.; Steinert, P.; Schäfer, M.; Werner, H. *J. Am. Chem. Soc.* **1993**, *115*, 9864–9865. (b) Wiedemann, R.; Wolf, J.; Werner, H. *J. Angew. Chem., Int. Ed. Engl.* **1995**, *34*, 1244–1246. (c) Wiedemann, R.; Wolf, J.; Werner, H. *J. Chem. Ber.* **1996**, *129*, 29–31. (d) Werner, H.; Wiedemann, R.; Steinert, P.; Wolf, J. *Chem. Eur. J.* **1997**, *3*, 127–137.



The successful preparation of the iridabenzvalenes can be attributed to the synergistic combination of intramolecular π bonding of the cyclopropene and σ -vinylic linkage to the Ir atom. By tethering of the strained ring through the vinyl group, the “effective concentration” of the cyclopropene moiety in the vicinity of the Ir center is high, leading to η^2 coordination. This is best exemplified by comparing the formation of **14d** with that of **18**. Whereas **14d** can be isolated in high yield,



reaction of 3,3-diphenylcyclopropene with $\text{IrCl(CO)(PEt}_3)_2$ shows only 40% conversion to **18** in solution, from which **18** can be isolated only as an inseparable 2:5 mixture with the starting Vaska complex.^{15f} Benzvalene formation also appears to be influenced by electronic factors. Although $\text{P}(i\text{-Bu})_3$ and PPh_3 are similar in size (cone angle of 143 vs 145°, respectively),²⁶ the former has considerably greater electron-donating ability and thus facilitates back-bonding from the metal center. Whereas **14a** is never observed, **14f** is the major product in the initially isolated mixture (ratio **14f**:**13f** = 2:1, Table 1). Only then do steric influences come into play, as the mixture isomerizes cleanly to **13g** overnight at room temperature.

Exactly how **14** “isomerizes” to **13** and how **13** forms in general are still subject to interpretation. If **14** is viewed as an iridabenzvalene, the simplest mechanistic explanation is a concerted rearrangement of the metallabicyclobutane moiety to give iridabenzene **13** directly (Scheme 6, path a). Such a concerted pathway was postulated for the thermally promoted isomerization of the purely hydrocarbon analogues.³² Alternatively, the isomerization of **14** may proceed in a stepwise fashion (path b), which is our preferred interpretation. Cyclopropene ligands in compounds prepared from Vaska-type iridium complexes (i.e., **18**) are relatively labile. For example, the cyclopropene in the PMe_3 analogue of **18** exchanges quantitatively at ambient temperatures

with a dideuterated version of the cyclopropene, or with electron-deficient olefins such as tetracyanoethylene and dimethyl maleate.^{15f} If the cyclopropene moiety of **14** dissociated from the Ir center, it would produce **17**, which is the same intermediate presumably formed in the initial step in Scheme 6. The σ -vinyl species **17** would also be the preferred complex in the equilibrium between **14** and **17** when larger and/or less donating phosphines are used. In the former case one can envisage a large degree of steric repulsion that would result between the bulky phosphine ligands and the cyclopropene phenyl groups when forming **14**. NMR experiments in our laboratory have shown that $\text{IrCl(CO)(PPh}_3)_2$ does not coordinate with **7** in benzene- d_6 at ambient temperature. Similarly, the equilibrium between 3,3-diphenylcyclopropene and Vaska’s complex lies exclusively to the side of the free cyclopropene.^{15f} Once formed, **17** would very likely be a highly reactive intermediate, considering that it is a coordinatively unsaturated, $16e^-$ species. Oxidative addition of the strained ring in **17** to the Ir center would give the metalla-Dewar benzene **19**. Rapid valence isomerization of **19** to iridabenzene **13** should be extremely facile because of the release of strain energy.

Missing from this mechanistic scheme is definitive evidence for the formation of **19**. Isomerization of **14** to **13** is a clean and quantitative process and, determined in the case of **14b**, proceeds with first-order kinetics. No other reaction products are observed in any of the NMR data. Similarly, only **13** is observed when larger and/or less donating phosphines are used. At the high temperatures (>50 °C) usually involved in the iridabenzvalene to iridabenzene rearrangement, **19** is not detected because, considering the high strain of the bicyclic system, it likely undergoes isomerization even more easily than **14**. Rearrangement of **19** is probably aided by larger phosphine ligands as well, which explains why this isomer is not observed in the room-temperature rearrangement of **14f** to **13f**.

Additional support for the metalla-Dewar benzene pathway involves a solvent effect. We have observed that the rate of rearrangement of **14** to **13** is faster in donating solvents than in nondonating solvents (e.g., **14d** is stable in benzene for more than a week but rearranges in acetone overnight).³⁰ It is known that donating solvents increase the rate of exchange of η^6 -coordinated arenes by assisting in the stepwise dissociation of the coordinated double bonds.²⁷ Accordingly, donation of an electron pair from acetone to the Ir center of **14** would likely assist the dissociation of the cyclopropene ligand, forming an unstable five-coordinate Ir(I) species. The acetone ligand could then dissociate, forming complex **17**. In a less donating solvent this $16e^-$ species intermediate would quickly re-form **14** (Scheme 6). Apparently, at ambient temperature in acetone, the “effective concentration” of **17** is sufficiently high that oxidative addition of the Ir to the cyclopropene σ -bond is preferred. Such a solvent effect would not be observed if “valence isomerization” proceeded via the concerted pathway. We are nevertheless actively working on metalla-Dewar benzene formation and characteriza-

(32) Christl, M. *Angew. Chem., Int. Ed. Engl.* **1981**, *20*, 529–546 and references therein.

tion.³³ Theoretical treatment of these extremely large metallacycles and of their mechanisms of interconversion is also underway.³⁴

Conclusion

In summary, we have prepared a family of iridabenzenes by the reaction of lithiated cyclopropene **16** with seven Vaska-type complexes. This novel, direct method into the metallabenzene manifold involves formation of a σ -bound vinylcyclopropene Ir(I) complex followed by an intramolecular Ir-mediated rearrangement of the strained ring. Use of small and/or electron-rich phosphines leads to the detection (**14c**, **14e**, **14f**) or isolation (**14b**, **14d**) of an intermediate valence isomer. This latter compound can be easily converted to the thermodynamically more stable benzene by heating in solution. X-ray data for **13a** and **13d** show the complexes to be essentially planar and fully delocalized in the bonding within the six-membered metallacycles. X-ray data for **14b** and **14d** reveal η^2 complexes possessing significant back-bonding from the metal and thus are best described as iridabenzvalenes. Mechanistic evidence suggests that the formation of the iridabenzenes, as well as isomerization of the iridabenzvalenes, goes through σ -bound species **17**, followed by oxidative addition to the strained ring, yielding the highly reactive irida-Dewar benzene **19**. Facile ring opening of this complex to **13** relieves ring strain and gains aromatic stabilization.

Our newly developed method represents only the third synthetic pathway to access heteroatom-free, nonstabilized metallaaromatics. We believe that this route will allow an augmented study of metallabenzenes for the following reasons. (1) Our route permits *direct access* into the metallabenzene manifold. There is no need for subsequent oxidative and/or reductive transformation(s) of the resultant organometallic species. If the metallabenzene does not form initially via our method, simple heating isomerizes the intermediate "valence isomer". (2) This route should permit the use of other transition-metal fragments. If so, our method would become the first *general pathway* to metallaaromatic formation. With the seven iridabenzenes reported in this paper, our route appears to be general using Vaska-type complexes. In addition, we have very recently extended this methodology to examples containing Rh^{12c} and Pt.^{12b} (3) Depending upon the cyclopropene used as the C₅ backbone, a variety of substituted metallacycles,^{12a} previously inaccessible substitution patterns, and new metallaaromatic topologies should become available. Work illustrating points 2 and 3 is currently in progress and will be reported shortly.

Experimental Section

General Considerations. (PPh₃)₂Ir(CO)Cl was purchased from Pressure Chemical Co. Bromomethyltriphenylphosphonium bromide and solutions of BuLi (2.5 M in hexanes) and NaN(SiMe₃)₂ (1.0 M in THF) were purchased from the Aldrich

Chemical Co. *N*-Methoxy-*N*-methyl-1,2-diphenyl-1-cyclopropene-3-carboxamide (**8**),¹⁸ iodomethyltriphenylphosphonium iodide,²⁰ and the remaining Vaska-type complexes²¹ were prepared according to the literature. Column chromatography was performed on Whatman reagent grade silica gel (230–400 mesh). Manipulation of organometallic reagents was carried out using either a Vacuum Atmospheres inert-atmosphere glovebox or standard Schlenk techniques. THF, Et₂O, toluene, and hexanes were distilled from Na/benzophenone and degassed by three freeze/pump/thaw cycles prior to use. NMR spectra were recorded on a Varian Unity-INOVA 300 spectrometer at ambient temperature. ¹H, ¹³C, and ³¹P NMR spectra were acquired at 299.95, 75.43, and 121.42 MHz, respectively. Chemical shifts for ¹H and ¹³C NMR spectra are reported in parts per million (δ) downfield from tetramethylsilane using the residual solvent signal (for CDCl₃, ¹H 7.26 and ¹³C 77.00; for CD₂Cl₂, ¹H 5.32 and ¹³C 54.00) as an internal standard. The ³¹P NMR spectrum is referenced relative to external H₃PO₄ or PPh₃. Coupling constants are reported in hertz. FT-IR spectra were recorded using a Nicolet Magna 550 FT-IR spectrometer. Melting points were determined using a Mel-Temp II capillary melting point apparatus equipped with a thermocouple and digital thermometer. Elemental analyses were performed by Robertson MicroLit Laboratories, Inc.

1,2-Diphenyl-1-cyclopropene-3-carbaldehyde (9). Amide **8**¹⁸ (3.60 g, 12.9 mmol) was dissolved in THF (200 mL) and cooled to -78 °C. LiAlH₄ (1.00 g, 26.6 mmol) was added in one portion and the resulting suspension stirred under N₂ at -78 °C for 5 h. Periodic monitoring of the reaction progress by TLC showed that the starting amide had been fully reduced during this period. Excess LiAlH₄ was quenched at -78 °C by the careful addition of 10% aqueous HCl solution (30 mL). Et₂O (50 mL) was added, the layers were separated, and the aqueous phase was extracted with an additional portion of Et₂O. The combined organics were washed successively with water, saturated NaHCO₃ solution, and brine. The organic layer was dried (MgSO₄), filtered, and concentrated to yield **9** (2.65 g, 93%) as a spectroscopically pure, light yellow solid. Mp: 81.9–82.6 °C. ¹H NMR (CDCl₃): δ 8.99 (d, J = 7.6 Hz, 1H), 7.72–7.68 (m, 4H), 7.54–7.42 (m, 6H), 2.96 (d, J = 7.6 Hz, 1H). ¹³C NMR (CDCl₃): δ 205.08, 129.95, 129.84, 129.05, 127.37, 107.55, 34.22. IR (KBr): 2937, 2789, 2710, 1697 cm⁻¹.

(E/Z)-1,2-Diphenyl-3-(2-bromoethenyl)-1-cyclopropene (10). Bromomethyltriphenylphosphonium bromide (120 mg, 0.275 mmol) was suspended in THF (10 mL) and cooled to -50 °C under an N₂ atmosphere. KO-*t*-Bu (30 mg, 0.267 mmol) was added in one portion, and the reaction mixture was stirred at -50 °C for 1 h. Aldehyde **9** (50 mg, 0.227 mmol) was dissolved in THF (1 mL) and added to the ylide using a syringe. After the mixture was stirred for 1 h at -50 °C, the cooling bath was removed and the mixture was stirred for an additional 12 h. Hexane (25 mL) was added, and the resulting thick suspension was filtered through Celite. The filter cake was washed with Et₂O and the solution concentrated to give an oily tan solid. The solid was purified by radial chromatography (9:1 hexanes/EtOAc, 2 mm rotor) to yield **10** (35 mg, 52%) as a pale yellow oil that was an inseparable 4:5 *E:Z* mixture of isomers. ¹H NMR (CDCl₃): δ 7.68 (d, J = 7.0 Hz, 4H), 7.48 (t, J = 7.5 Hz, 4H), 7.38 (t, J = 7.4 Hz, 2H), 6.27 (d, J = 13.6 Hz, 1H (*E*)), 6.17 (d, J = 7.4 Hz, 1H (*Z*)), 6.04 (dd, J = 13.6, 7.8 Hz, 1H (*E*)), 5.81 (t, J = 7.4 Hz, 1H (*Z*)), 3.14 (d, J = 7.8 Hz, 1H (*Z*)), 2.79 (d, J = 7.4 Hz, 1H (*E*)).

(Z)-1,2-Diphenyl-3-(2-iodoethenyl)-1-cyclopropene (7). Iodomethyltriphenylphosphonium iodide²⁰ (2.95 g, 5.57 mmol) was suspended in THF (11 mL). A solution of NaN(SiMe₃)₂ in THF (5.6 mL, 1.0 M, 5.6 mmol) was added via syringe, and the suspension immediately turned yellow. After it was stirred at ambient temperature for 5 min, the yellow mixture was then cooled to -78 °C and HMPA (1.5 mL) was added via syringe. Aldehyde **9** (1.23 g, 5.60 mmol) was dissolved in THF (1 mL) and added to the ylide via syringe. The temperature was

(33) After this study, we have prepared repeatedly in good yield what we believe is a rhoda-Dewar benzene from RhCl(cod)P(*i*-Pr)₃ and **16**. The ¹H, ¹³C, and ³¹P NMR data all support such a structure. We are currently attempting to obtain an X-ray crystal structure: Wu, H.-P.; Haley, M. M. Unpublished results.

(34) Williams, R. V.; Braden, D. A.; Haley, M. M. Unpublished results.

increased to $-30\text{ }^{\circ}\text{C}$ (*o*-xylene/liquid N_2), and the reaction mixture was stirred for 45 min. Analysis by TLC showed no aldehyde remaining after this period. Et_2O (75 mL) was added, resulting in a thick suspension. The suspension was filtered, and the filter cake was washed with Et_2O . The filtrate was washed successively with 10% HCl solution, water, saturated NaHCO_3 solution, and brine. The organic phase was dried (MgSO_4), filtered, and concentrated to give an oily brown solid. Chromatography on silica gel (9:1 hexanes/ EtOAc) yielded **7** (1.56 g, 81%) as a light yellow solid. The vinyl iodide was stored with a small amount (~ 1 mg) of hydroquinone to prevent decomposition. Mp: $74.2\text{--}75.6\text{ }^{\circ}\text{C}$. ^1H NMR (CDCl_3): δ 7.69 (d, $J = 7.5$ Hz, 4H), 7.49 (t, $J = 7.5$ Hz, 4H), 7.39 (t, $J = 7.5$ Hz, 2H), 6.14 (d, $J = 7.5$ Hz, 1H), 5.92 (t, $J = 7.5$ Hz, 1H), 3.01 (d, $J = 7.5$ Hz, 1H). ^{13}C NMR (CDCl_3): δ 144.58, 129.69, 128.91, 128.84, 128.71, 113.32, 77.29, 27.01. IR (KBr): 1833 cm^{-1} (cyclopropene). Anal. Calcd for $\text{C}_{17}\text{H}_{13}\text{I}$: C, 59.32; H, 3.81. Found: C, 59.23; H, 4.02.

(Z)-3-(2,3-Diphenylcycloprop-2-enyl)propenoic acid (11). Cyclopropene **7** (40 mg, 0.12 mmol) was dissolved in Et_2O (5 mL) and cooled to $-78\text{ }^{\circ}\text{C}$ under an N_2 atmosphere. A hexanes solution of *t*-BuLi (0.14 mL, 1.7 M, 0.24 mmol) was added over 1 min via syringe. The resulting pale yellow solution was stirred at $-78\text{ }^{\circ}\text{C}$ for 15 min, and then dry CO_2 gas was passed through the solution for 15 min. The mixture was warmed to room temperature and the reaction quenched by addition of 10% HCl solution and Et_2O . The organic layer was washed sequentially with H_2O and brine, dried (MgSO_4), and concentrated. Recrystallization of the crude solid from CHCl_3 gave **11** (22 mg, 81%) as a white powder. Mp: $172.4\text{--}173.3\text{ }^{\circ}\text{C}$. ^1H NMR (CDCl_3): δ 7.68 (d, $J = 7.3$ Hz, 4H), 7.48 (t, $J = 7.5$ Hz, 4H), 7.38 (t, $J = 7.5$ Hz, 2H), 6.04 (dd, $J = 11.4, 9.5$ Hz, 1H), 5.85 (d, $J = 11.4$ Hz, 1H), 3.99 (d, $J = 9.5$ Hz, 1H). ^{13}C NMR (CDCl_3): δ 160.71, 129.69, 129.04, 128.87, 128.63, 117.37, 113.42, 22.62. IR (KBr): 3080, 3059, 3030, 1689, 1611, 1445 cm^{-1} . Anal. Calcd for $\text{C}_{18}\text{H}_{14}\text{O}_2$: C, 82.42; H, 5.38. Found: C, 82.31; H, 5.52.

General Metallacycle Synthesis. A flame-dried Schlenk flask was charged with cyclopropene **7** (186 mg, 0.54 mmol) and Et_2O (5 mL). The solution was cooled to $-78\text{ }^{\circ}\text{C}$ under an Ar atmosphere, and a hexane solution of BuLi (0.21 mL, 2.5 M, 0.53 mmol) was added via syringe. The resulting solution was stirred at $-78\text{ }^{\circ}\text{C}$ for 10 min, and then a solution of $\text{IrCl}(\text{CO})(\text{PR}_3)_2$ (0.5 mmol) in toluene (10 mL) precooled to $-78\text{ }^{\circ}\text{C}$ was added over a 2 min period using a double-ended needle under Ar pressure. The solution was stirred at $-78\text{ }^{\circ}\text{C}$ for 10 min and then allowed to equilibrate to ambient temperature over a 1 h period. The color of the solution changed from yellow to orange/orange-red during this period, and a white precipitate of LiCl was formed. CHCl_3 (0.10 mL) was added by syringe, the suspension was filtered through a glass frit of medium porosity, and the solvent was removed in vacuo. The residue was purified by column chromatography and/or recrystallized to give either iridabenzenes **13a,c,e,g** or iridabenzvalenes **14b,d**. Despite numerous attempts, iridabenzene **13f** never crystallized.

Iridabenzene 13a (PPh₃). $\text{IrCl}(\text{CO})(\text{PPh}_3)_2$ (390 mg, 0.5 mmol) gave a red powder by following the general procedure. The material was dissolved in toluene, and hexane was carefully added. After it was cooled to $-35\text{ }^{\circ}\text{C}$ overnight, the solution yielded **13a** (318 mg, 66%) as red prisms. Mp: $196\text{--}198\text{ }^{\circ}\text{C}$ (sealed tube under Ar). ^1H NMR (CD_2Cl_2): δ 10.41 (ddt, $J = 11.4, 10.2, 1.2$ Hz, *H5*), 7.99 (ddt, $J = 7.5, 6.0, 1.2$ Hz, *H3*), 7.69 (dd, $J = 10.2, 7.5$ Hz, *H4*), 7.30 (d, $J = 8.1$ Hz, 2H), 7.24–7.15 (m, 16H), 7.09–6.83 (m, 21H), 6.71 (t, $J = 7.5$ Hz, 1H). ^{13}C NMR (CD_2Cl_2): δ 201.09 (t, $J = 50.5$ Hz, CO), 187.60 (t, $J = 7.0$ Hz, C1), 187.43 (s, C5), 169.09 (t, $J = 3.6$ Hz), 147.59 (t, $J = 4.1$ Hz), 141.93 (t, $J = 6.0$ Hz, C2), 139.99 (t, $J = 8.0$ Hz, C3), 135.85 (m, PPh₃), 134.49 (t, $J = 5.5$ Hz, PPh₃), 131.70 (s), 130.16 (s, PPh₃), 128.33 (t, $J = 5.0$ Hz, PPh₃), 127.76 (t, $J = 4.1$ Hz, C4), 127.12 (s), 125.84 (s), 124.81 (s), 124.71 (t, $J =$

6.5 Hz), 122.77 (s). ^{31}P NMR (CD_2Cl_2): δ 16.44 (s). IR (KBr): 1990 cm^{-1} (CO). Anal. Calcd for $\text{C}_{54}\text{H}_{43}\text{IrOP}_2$: C, 67.41; H, 4.50. Found: C, 67.23; H, 4.41.

Iridabenzene 13b and Iridabenzvalene 14b (PMe₃). $\text{IrCl}(\text{CO})(\text{PMe}_3)_2$ (204 mg, 0.5 mmol) gave an orange oil by following the general procedure. ^1H NMR of the crude material showed exclusive formation of **14b**. The oil was diluted with minimal Et_2O and cooled to $-35\text{ }^{\circ}\text{C}$, providing **14b** (159 mg, 54%) as light yellow crystals. Spectroscopic data for pure **14b** have been described previously.¹¹

Conversion to **13b** could be accomplished by dissolving **14b** (59 mg, 0.10 mmol) in toluene (5 mL) and heating overnight at $75\text{ }^{\circ}\text{C}$. Solvent was removed in vacuo to give a deep red solid, which was taken up in Et_2O . The ethereal solution was cooled to $-35\text{ }^{\circ}\text{C}$, whereupon **13b** (57 mg, 97%) deposited as red-orange crystals. For accurate comparison, all NMR data were reacquired in CD_2Cl_2 . ^1H NMR (CD_2Cl_2): δ 11.10 (ddt, $J = 12.2, 10.1, 1.2$ Hz, *H5*), 7.75 (ddt, $J = 8.0, 6.1, 1.2$ Hz, *H3*), 7.49 (ddt, $J = 10.1, 8.0, 0.9$ Hz, *H4*), 7.08–6.93 (m, 9H), 6.77 (t, $J = 6.9$ Hz, 1H), 1.62 (d, $J = 10.2$ Hz, 18H). ^{13}C NMR (CD_2Cl_2): δ 189.44 (t, $J = 50.4$ Hz, CO), 189.25 (t, $J = 5.5$ Hz, C1), 176.58 (s, C5), 168.39 (t, $J = 3.2$ Hz), 148.59 (t, $J = 4.0$ Hz), 140.49 (t, $J = 5.0$ Hz, C2), 135.53 (t, $J = 8.3$ Hz, C3), 131.50 (s), 128.65 (t, $J = 4.3$ Hz, C4), 126.99 (s), 126.21 (t, $J = 6.0$ Hz), 125.57 (s), 124.39 (s), 122.70 (s), 21.39 (d, $J = 36.1$ Hz, P(CH₃)₃). ^{31}P NMR (CD_2Cl_2): δ -40.54 (s). IR (CD_2Cl_2 solution/CaF cell): 1962 cm^{-1} (CO). All other data were previously described.¹¹

Iridabenzene 13c and Iridabenzvalene 14c (PMe₂Ph). $\text{IrCl}(\text{CO})(\text{PMe}_2\text{Ph})_2$ (266 mg, 0.5 mmol) gave an orange oil by following the general procedure. ^1H NMR of the crude material showed formation of 2:98 mixture of **13c:14c** along with protonated vinylcyclopropene. Diagnostic peaks for **14c** are as follows. ^1H NMR (C_6D_6): δ 7.58 (d, $J = 6.9$ Hz, 4H), 7.32–7.30 (m, 4H), 7.20–6.90 (m, 13H), 6.62 (ddt, $J = 8.7, 8.4, 2.7$ Hz, *H4*), 3.80–3.76 (m, *H3*), 1.38 (br d, $J = 8.7$ Hz, 6H), 1.31 (br d, $J = 8.7$ Hz, 6H). ^{31}P NMR (C_6D_6): δ -32.89 (s).

Column chromatography (Et_2O) of the crude oil in the glovebox removed the remaining starting iridium salt. Addition of petroleum ether and cooling to $-20\text{ }^{\circ}\text{C}$ provided **13c** (207 mg, 58%) as red crystals. All attempts to purify **14c** resulted in isomerization and isolation instead of pure **13c**. ^1H NMR (CD_2Cl_2): δ 11.05 (dq, $J = 11.4, 1.2$ Hz, *H5*), 7.82 (ddt, $J = 8.2, 5.9, 1.2$ Hz, *H3*), 7.57–7.49 (m, *H4*), 7.39–7.21 (m, 10H), 7.04–6.86 (m, 9H), 6.74 (t, $J = 7.0$ Hz, 1H), 1.66 (d, $J = 10.0$ Hz, 6H), 1.62 (d, $J = 10.0$ Hz, 6H). ^{13}C NMR (CD_2Cl_2): δ 190.77 (t, $J = 50.5$ Hz, CO), 188.56 (t, $J = 6.0$ Hz, C1), 179.68 (s, C5), 168.18 (t, $J = 3.4$ Hz), 148.32 (t, $J = 4.2$ Hz), 140.53 (t, $J = 4.5$ Hz, C2), 136.49 (t, $J = 8.5$ Hz, C3), 131.44 (s), 130.60 (t, $J = 5.0$ Hz), 129.93 (s), 128.85 (t, $J = 4.0$ Hz, C4), 128.72 (t, $J = 5.0$ Hz), 127.02 (s), 125.98 (t, $J = 5.5$ Hz), 125.61 (s), 124.46 (s), 122.91 (s), 16.42 (m). ^{31}P NMR (CD_2Cl_2): δ -26.90 (s). IR (CD_2Cl_2 solution/CaF cell): 1970 cm^{-1} (CO). Anal. Calcd for $\text{C}_{34}\text{H}_{35}\text{IrOP}_2$: C, 57.21; H, 4.94. Found: C, 57.08; H, 4.72.

Iridabenzene 13d and Iridabenzvalene 14d (PET₃). $\text{IrCl}(\text{CO})(\text{PET}_3)_2$ (246 mg, 0.5 mmol) gave an orange oil by following the general procedure. ^1H NMR of the crude material showed exclusive formation of **14d**. The oil was diluted with minimal Et_2O and cooled to $-35\text{ }^{\circ}\text{C}$, providing **14d** (171 mg, 51%) as light yellow crystals. ^1H NMR (C_6D_6): δ 7.72 (d, $J = 7.3$ Hz, 4H), 7.21 (t, $J = 7.3$ Hz, 4H), 7.07 (ddt, $J = 8.2, 4.4, 2.1$ Hz, *H5*), 6.98 (t, $J = 7.3$ Hz, 2H), 6.74 (ddt, $J = 8.2, 7.8, 2.6$ Hz, *H4*), 3.73–3.67 (m, *H3*), 1.71–1.43 (m, 12H), 0.76 (dt, $J = 14.9, 7.6$ Hz, 18H). ^{13}C NMR (C_6D_6): δ 181.90 (t, $J = 7.1$ Hz), 147.22 (t, $J = 3.5$ Hz), 145.18 (t, $J = 7.1$ Hz), 140.84 (t, $J = 15.1$ Hz), 128.52 (s), 124.62 (s), 67.78 (m), 59.66 (t, $J = 3.5$ Hz), 21.23 (m), 8.12 (s). ^{31}P NMR (C_6D_6): δ -20.85 (s). IR (KBr): 1961 cm^{-1} (CO). Anal. Calcd for $\text{C}_{30}\text{H}_{43}\text{IrOP}_2$: C, 53.47; H, 6.43. Found: C, 53.21; H, 6.53.

Conversion to **13d** could be accomplished by dissolving **14d** (101 mg, 0.15 mmol) in toluene (8 mL) and heating overnight

at 75 °C. Solvent was removed in vacuo to give a deep red solid, which was taken up in Et₂O. The ethereal solution was cooled to -35 °C, whereupon **13d** (96 mg, 95%) deposited as red-orange crystals. ¹H NMR (CD₂Cl₂): δ 11.30 (ddt, *J* = 10.8, 10.1, 1.2 Hz, *H5*), 7.69 (ddt, *J* = 7.8, 6.5, 1.3 Hz, *H3*), 7.40 (dd, *J* = 10.1, 7.8 Hz, *H4*), 7.04–6.89 (m, 9H), 6.76–6.71 (m, 1H), 1.92–1.79 (m, 12H), 0.96–0.85 (m, 18H). ¹³C NMR (CD₂Cl₂): δ 192.36 (t, *J* = 48.8 Hz, CO), 189.87 (t, *J* = 6.4 Hz, C1), 176.45 (s, C5), 168.06 (t, *J* = 3.3 Hz), 148.65 (t, *J* = 4.1 Hz), 140.53 (t, *J* = 5.0 Hz, C2), 135.67 (t, *J* = 8.0 Hz, C3), 131.50 (s), 128.07 (t, *J* = 4.1 Hz, C4), 126.93 (s), 126.56 (t, *J* = 5.0 Hz), 125.38 (s), 124.26 (s), 122.64 (s), 21.90 (m), 8.66 (s). ³¹P NMR (C₆D₆): δ -0.91 (s). IR (CD₂Cl₂ solution/CaF cell): 1967 cm⁻¹ (CO). Anal. Calcd for C₃₀H₄₃IrOP₂: C, 53.47; H, 6.43. Found: C, 53.62; H, 6.37.

Iridabenzene 13e and Iridabenzvalene 14e (PMePh₂). IrCl(CO)(PMePh₂)₂ (328 mg, 0.5 mmol) gave a red-orange oil by following the general procedure. ¹H NMR analysis of the crude material showed formation of a 30:70 mixture of **13e** and **14e** along with protonated vinylcyclopropene. Partial NMR data for **14e** are as follows. ¹H NMR (C₆D₆): δ 7.53 (d, *J* = 7.2 Hz, 4H), 6.82–6.76 (m, *H4*), 4.00–3.95 (m, *H3*). ³¹P NMR (C₆D₆): δ -24.12.

Column chromatography (Et₂O) of the crude oil in the glovebox removed the remaining starting iridium salt. Addition of petroleum ether and cooling to -20 °C provided **13e** (234 mg, 56%) as red crystals. All attempts to purify **14e** resulted in facile isomerization and isolation instead of pure **13e**. Mp: 79.6–81.2 °C (sealed tube under Ar). ¹H NMR (CD₂Cl₂): δ 10.93 (dq, *J* = 10.6, 1.2 Hz, *H5*), 7.98 (ddt, *J* = 7.9, 6.2, 1.2 Hz, *H3*), 7.66 (dd, *J* = 10.0, 7.9 Hz, *H4*), 7.29–7.01 (m, 20H), 6.85 (t, *J* = 7.5 Hz, 4H), 6.75 (d, *J* = 6.7 Hz, 4H), 6.66 (t, *J* = 7.2 Hz, 2H), 1.84 (d, *J* = 9.4 Hz, 6H). ¹³C NMR (CD₂Cl₂): δ 197.14 (t, *J* = 52.5 Hz, CO), 187.36 (t, *J* = 6.5 Hz, C1), 181.93 (s, C5), 168.97 (t, *J* = 3.1 Hz), 148.00 (t, *J* = 4.1 Hz), 141.47 (t, *J* = 6.1 Hz, C2), 137.61 (t, *J* = 8.5 Hz, C3), 134.49 (m), 132.50 (t, *J* = 5.5 Hz), 131.69 (s), 130.14 (s), 128.44 (t, *J* = 4.5 Hz), 128.37 (t, *J* = 4.5 Hz, C4), 127.05 (s), 125.65 (s), 125.11 (t, *J* = 6.0 Hz), 124.67 (s), 122.67 (s), 18.25 (m). ³¹P NMR (CD₂Cl₂): δ -5.20 (s). IR (CD₂Cl₂ solution/CaF cell): 1979 cm⁻¹ (CO). Anal. Calcd for C₄₄H₃₉IrOP₂: C, 63.07; H, 4.69. Found: C, 62.94; H, 4.47.

Iridabenzene 13f and Iridabenzvalene 14f (P(*i*-Bu)₃). IrCl(CO)[P(*i*-Bu)₃]₂ (330 mg, 0.5 mmol) gave a red-orange oil by following the general procedure. ¹H NMR analysis of the crude material showed formation of a 35:65 mixture of **13f** and **14f** along with protonated vinylcyclopropene. Partial NMR data for **14f** are as follows. ¹H NMR (C₆D₆): δ 7.66 (d, *J* = 7.5 Hz, 4H), 6.92–6.88 (m, *H4*), 3.73–3.68 (m, *H3*). ³¹P NMR (C₆D₆): δ -19.70 (s).

Column chromatography (pentane) of the crude oil in the glovebox removed the remaining starting iridium salt. The pentane fractions were concentrated to one-fourth volume and cooled to -78 °C; however, all attempts to prepare crystalline material were unsuccessful. Removal of the solvent provided **13f** (207 mg, 49%) as an oxygen-sensitive, dark red oil. ¹H NMR (CD₂Cl₂): δ 10.89 (dq, *J* = 10.0, 1.2 Hz, *H5*), 7.71 (ddt, *J* = 7.6, 5.9, 1.2 Hz, *H3*), 7.51 (dd, *J* = 10.3, 7.6 Hz, *H4*), 7.04–6.84 (m, 9H), 6.70 (t, *J* = 7.0 Hz, 1H), 2.01–1.78 (m, 12H), 1.72 (sep, *J* = 6.2 Hz, 6H), 0.96 (d, *J* = 6.4 Hz, 18H), 0.90 (d, *J* = 6.4 Hz, 18H). ¹³C NMR (CD₂Cl₂): δ 194.09 (t, *J* = 50.2 Hz, CO), 190.54 (t, *J* = 5.5 Hz, C1), 177.28 (s, C5), 169.01 (t, *J* = 3.6 Hz), 148.67 (t, *J* = 4.0 Hz), 141.45 (t, *J* = 5.5 Hz, C2), 136.14 (t, *J* = 8.0 Hz, C3), 131.66 (s), 128.01 (t, *J* = 4.5 Hz, C4), 126.88 (s), 125.88 (t, *J* = 6.0 Hz), 125.41 (s), 124.30 (s), 122.18 (s), 40.59 qu, *J* = 10.6 Hz), 25.85 (m). ³¹P NMR (CD₂Cl₂): δ -0.29 (s). IR (CD₂Cl₂ solution/CaF cell): 1958 cm⁻¹ (CO).

Iridabenzene 13g (P(*p*-MeOPh)₃). IrCl(CO)[P(*p*-MeOPh)₃]₂ (480 mg, 0.5 mmol) gave a red powder following the general procedure. The material was dissolved in toluene and filtered

Table 6. Crystal Data for Compounds 13d, 14d, and 15

	13d	14d	15
mol formula	C ₃₀ H ₄₃ IrOP ₂	C ₃₀ H ₄₃ IrOP ₂	C ₂₄ H ₃₁ IrO ₃ P ₂
mol wt	673.84	673.84	621.68
cryst syst	monoclinic	orthorhombic	monoclinic
space group	<i>C2/c</i>	<i>P2₁2₁2₁</i>	<i>P2₁/n</i>
<i>a</i> (Å)	35.155(4)	11.190(1)	9.248(4)
<i>b</i> (Å)	10.9765(12)	14.014(3)	12.4422(13)
<i>c</i> (Å)	15.3910(16)	18.878(2)	21.713(3)
<i>α</i> (deg)	90	90	90
<i>β</i> (deg)	95.615(9)	90	90.98(2)
<i>γ</i> (deg)	90	90	90
<i>V</i> (Å ³)	5911(1)	2960.3(8)	2498(1)
<i>Z</i>	8	4	4
2 θ _{max} (deg)	50	55	50
no. of indep rflns	5373	3818	4629
no. of obsd rflns	3644	3037	3333
(<i>I</i> ≥ <i>σ</i> (<i>I</i>))			
no. of rflns used in refinement	5104	3792	4400
<i>F</i> ₀₀₀	2704	1352	1224
no. of refined params	293	307	271
<i>R</i> (<i>F</i>)/ <i>R</i> _w (<i>I</i> ≥ <i>σ</i> (<i>I</i>))	0.044/0.043	0.039/0.041	0.037/0.036
<i>R</i> (<i>F</i> ²)/ <i>R</i> _w (<i>F</i> ²) (all)	0.075/0.105	0.074/0.090	0.058/0.077

through Celite. Hexane was carefully added and the solution cooled overnight at -35 °C, yielding **13g** (348 mg, 61%) as red prisms. Mp: 133.8–135.6 °C (sealed tube under Ar). ¹H NMR (CD₂Cl₂): δ 10.43 (dq, *J* = 10.2, 1.1 Hz, *H5*), 7.96 (ddt, *J* = 7.8, 6.4, 1.1 Hz, *H3*), 7.38 (dd, *J* = 10.1, 7.8 Hz, *H4*), 7.08 (d, *J* = 4.4 Hz, 4H), 7.01–6.81 (m, 15H), 6.77–6.66 (m, 15H), 3.79 (s, 18H). ¹³C NMR (CD₂Cl₂): δ 198.18 (t, *J* = 52.0 Hz, CO), 188.51 (t, *J* = 6.5 Hz, C1), 187.11 (s, C5), 169.25 (t, *J* = 3.0 Hz), 161.16 (s), 147.88 (t, *J* = 4.1 Hz), 141.70 (t, *J* = 5.5 Hz, C2), 138.92 (t, *J* = 8.5 Hz, C3), 135.92 (t, *J* = 6.0 Hz), 131.75 (s), 128.50 (t, *J* = 5.0 Hz, C4), 127.06 (s), 125.74 (s), 124.91 (t, *J* = 6.5 Hz), 124.69 (s), 122.58 (s), 113.61 (t, *J* = 5.5 Hz), 55.79 (s). ³¹P NMR (CD₂Cl₂): δ 13.01 (s). IR (KBr): 1973 cm⁻¹ (CO). Anal. Calcd for C₄₄H₃₉IrOP₂: C, 63.07; H, 4.69. Found: C, 62.84; H, 4.57.

Dioxygen Cycloadduct 15. Iridabenzene **13a** (59 mg, 0.10 mmol) was dissolved in benzene (5 mL) and Et₂O (5 mL) and the deep red solution stirred open to the air for 5 min with a color change to pale yellow. The solution was cooled at -30 °C overnight, yielding **15** (51 mg, 82%) as yellow crystals. ¹H NMR (CDCl₃): δ 7.75 (ddt, *J* = 15.5, 9.0 Hz, 1.2 Hz, *H5*), 7.08–6.87 (m, 11H), 5.09 (d, *J* = 6.5 Hz, *H3*), 1.56 (d, *J* = 9.8 Hz, 9H), 1.29 (d, *J* = 10.5 Hz, 9H). ¹³C NMR (C₆D₆): δ 175.20 (t, *J* = 6.1 Hz), 153.58 (s), 147.38 (dd, *J* = 89.7, 6.0 Hz), 145.46 (t, *J* = 9.1 Hz), 145.03 (d, *J* = 9.1 Hz), 135.75 (s), 129.66 (d, *J* = 2.0 Hz), 129.58 (s), 127.39 (d, *J* = 3.0 Hz), 127.32 (s), 124.61 (s), 124.21 (s), 90.30 (s, C3), 17.86 (d, *J* = 40.3 Hz), 14.33 (d, *J* = 31.2 Hz). ³¹P NMR (C₆D₆): δ -40.40 (d, *J* = 9.5 Hz), -35.70 (d, *J* = 9.5 Hz). IR (CH₂Cl₂): 2013 (s, CO) cm⁻¹. Anal. Calcd for C₂₄H₃₁IrO₃P₂: C, 46.55; H, 4.88. Found: C, 46.37; H, 5.03.

X-ray Structure Determinations. Data were collected on an Enraf-Nonius CAD-4 Turbo diffractometer using Mo K α radiation: λ = 0.710 73 Å; graphite monochromator; *T* = 296 K; scan mode ω -2 θ . Pertinent crystallographic data and refinement parameters are given in Table 6. Structure refinement (C atoms anisotropic, H atoms riding) was accomplished with the teXsan program suite (version 1.7 for SGI workstations). Further details are contained in the Supporting Information.

Acknowledgment. This research has been supported by the National Science Foundation (Grant No. CHE-0075246) and The Camille and Henry Dreyfus Foundation (Teacher-Scholar Award 1998–2003 to

M.M.H.). We thank Dr. Alex Blumenfeld (University of Idaho) for acquisition of the HMBC and HMQC NMR spectra, Dr. Volker Jacob and A. J. Boydston for acquisition of some characterization data, Prof. John Bleeke regarding details of the crystal structure of **1·O₂**, and Profs. Ken Doxsee, Jim Hutchison, and David Tyler for helpful discussions.

Supporting Information Available: Figures giving X-ray crystal structures and tables of atomic coordinates, thermal parameters, bond lengths and bond angles for **13d**, **14d**, and **15**. This material is available free of charge via the Internet at <http://pubs.acs.org>.

OM030394D